

# Nonlinear FE modelling and parametric study on flexural performance of ECC beams

Hind M. Kh<sup>\*</sup>, Mustafa Özakça<sup>a</sup> and Talha Ekmekyapar<sup>b</sup>

Department of Civil Engineering, University of Gaziantep, 27310 Gaziantep, Turkey

(Received October 24, 2015, Revised September 5, 2016, Accepted November 15, 2016)

**Abstract.** Engineered Cementitious Composite (ECC) is a special class of the new generation of high performance fiber reinforced cementitious composites (HPFRCC) featuring high ductility with relatively low fiber content. In this research, the mechanical performance of ECC beams will be investigated with respect to the effect of slag and aggregate size and amount, by employing nonlinear finite element method. The validity of the models was verified with the experimental results of the ECC beams under monotonic loading. Based on the numerical analysis method, nonlinear parametric study was then conducted to evaluate the influence of the ECC aggregate content (AC), ECC compressive strength ( $f_{ECC}$ ), maximum aggregate size ( $D_{max}$ ) and slag amount ( $\phi$ ) parameters on the flexural stress, deflection, load and strain of ECC beams. The simulation results indicated that when increase the slag and aggregate size and content no definite trend in flexural strength is observed and the ductility of ECC is negatively influenced by the increase of slag and aggregate size and content. Also, the ECC beams revealed enhancement in terms of flexural stress, strain, and midspan deflection when compared with the reference beam (microsilica MSC), where, the average improvement percentage of the specimens were 61.55%, 725%, and 879%, respectively. These results are quite similar to that of the experimental results, which provides that the finite element model is in accordance with the desirable flexural behaviour of the ECC beams. Furthermore, the proposed models can be used to predict the flexural behaviour of ECC beams with great accuracy.

**Keywords:** engineered cementitious composite (ECC); flexural behavior; ductility; finite element modelling; parametric study

## 1. Introduction

In recent years, the effort to modify the brittle nature of ordinary concrete has resulted in modern concepts of high performance fiber reinforced cementitious composites, which are characterized by tensile strain-hardening after first cracking. Depending on its composition, its tensile strain capacity can be up to several hundred times those of normal and fiber reinforced concrete (Balaguru and Shah 1992, Lim and Li 1997, Kunieda and Rokugo 2006, Fraternali *et al.* 2011, Cho *et al.* 2012, D'Ambrisi *et al.* 2012, D'Ambrisi *et al.* 2013).

Recently, engineered cementitious composites (ECCs) have been proposed as a new class of concrete materials which have considerably greater level of ductility.

ECC is a unique kind of cementitious composite having high ductility and damage tolerance properties under intense mechanical loadings, including tensile and shear loadings (Li 1998, Li *et al.* 2001, Li 2002, Zhang and Li 2002, Lepech and Li 2008, Li 2008, Sahmaran and Li 2009).

The material is optimized as per the principles of

micromechanics (Li 1993, Maalej and Li 1995, Lin and Li 1997, Li 1998, Zhang *et al.* 2006, Hawileh 2015) which increases the tensile strain capacity of material up to 3-5% where operating uniaxial tensile loading making it achievable through only 2% polyvinyl alcohol (PVA) or polyethylene fibre (PE) quantity by volume (Li *et al.* 1995, Li 1998, Lin *et al.* 1999, Maruta *et al.* 2005). The characteristic strain-hardening behavior of ECC is accompanied by the sequential development of multiple microcracking. Even at ultimate load, the crack width remains on the order of 50 to 80  $\mu\text{m}$ .

A micromechanics-based material design theory is employed to enhance the strength and energy ratios of the mixture proportions of ECC to acquire high composite ductility (Li 1998, Li *et al.* 2001, Dhawale and Joshi 2013). The crack control properties of ECCs with respect to controlling the width of occurring cracks depend upon the type, size, and amount of fibre, matrix ingredients and interface properties of the material. The manufacture of ECCs is done by employing particular quantities of high-quality mixtures, which when accompanied by the bristly material in the paste, helps to enhance the matrix (ECC without fibre) toughness. As a result, the material attains the crack control characteristics i.e., delayed crack initiation and prevention of steady-state flat-crack propagation which might cause to reduce the tensile ductility of ECC (Nallathambi *et al.* 1984, Li *et al.* 1995, Perdikaris and Romeo 1995). Moreover, the introduction of aggregates with a particle size larger than the average fiber spacing

\*Corresponding author, Assistant Professor

E-mail: hindmahmood18@gmail.com

<sup>a</sup>Professor

<sup>b</sup>Assistant Professor

leads to balling of fibers and results in poor fiber dispersion uniformity (Nagi, M. and Hsu 1992, De Koker and Van Zijl 2004). This proposes that ECC with fine aggregate must have a standard aggregate/binder ratio (A/B) of 0.36 and a maximum grain size of 250  $\mu\text{m}$  (Hind *et al.* 2016b, c, d, Li *et al.* 1995, Fischer and Li 2003).

Due to environmental and economical reasons, there is a growing trend toward using industrial by-products as supplementary materials in the production of different types of concrete mixtures. Among the various supplementary materials, Slag (*S*) is the most commonly available mineral admixture. This by-products from industrial processes is usually available in large quantities. However, in the past few years, *S* has been used as a substitution of cement with regard to its application in ECC (Kim *et al.* 2007, Wang and Li 2007, Zhou *et al.* 2010). Higher concentration of cement is obtained when coarse aggregate is absent in ECC. Furthermore, partial replacement helps to reduce ecological loadings. As mentioned previously, employing larger quantities of mineral admixtures, helps decreasing the strength of matrix while enhancing that of ECC with respect to tensile ductility (Wang and Li 2007, Yang *et al.* 2009, Nematollahi *et al.* 2015). Moreover, anhydrite mineral admixtures having small particle size and even spherical shape are employed as filler particles, providing higher density of the fibre/matrix interface transition zone resulting to produce high frictional bonding (Wang and Li 2007, Pan *et al.* 2015, Said and Razak 2015, Said *et al.* 2015). This enhances long-term stability of the structure by significantly decreasing the steady-state crack width.

It is hypothesized that the increase in matrix toughness due to an increased amount and size of aggregates could potentially be offset by the decrease in toughness when high-volume mineral admixture is used in the production of ECC. Recently, Sahmaran *et al.* (Şahmaran *et al.* 2009, Şahmaran *et al.* 2013) investigated the influence of aggregate size on the mechanical properties of high-volume FA-ECC. The test results indicate that aggregates with a maximum aggregate size of up to 2.38 mm, as long as they do not interfere with the uniform fiber dispersion, do not negatively influence the ductility of ECC. In addition to aggregate size, there is a desire to increase the amount of aggregates and explore the use of an alternative mineral admixture type beyond FA. However, far too little attention has been paid to study the flexural behavior of the ECC beams numerically. In addition, the influence of using slag as a deliberate approach has also not studied in terms of limit the matrix toughness and restore tensile ductility when higher amounts of aggregates are used. This study intends to fill this knowledge gap.

The objective of this study is to investigate the influence of simultaneously increasing the aggregate amount and size and slag amount on the flexural behavior of the ECC beams using 3D nonlinear finite element simulation by ANSYS software. The comparative analysis of these results with those obtained through experimental study of elements having similar geometric and mechanical characteristics, employing them as reference models. A nonlinear parametric study was conducted to examine the influence of the ECC aggregate content (*AC*), ECC compressive strength

( $f_{ECC}$ ), maximum aggregate size ( $D_{max}$ ) and slag amount ( $\phi$ ) factors on the flexural stress, deflection, load and strain.

## 2. Numerical modelling of ECC beams

### 2.1 ANSYS finite element models

ANSYS program was employed to determine the malfunctioning of nonlinear finite element model. The program is able to deal with the particular numerical models designed to account for the nonlinear course of actions of concrete and ECC beams operating under invariable loadings. The ECC beams and Microsilica concrete (MSC) were modelled by using SOLID 65 elements. Each of these elements entails eight nodes with three levels of freedom at each node and transformations in the nodal *x*-, *y*- and *z*-directions. SOLID 65 elements hold the properties of plastic deformation, three-dimensional cracking and crushing. ANSYS employs linear isotropic and multi-linear isotropic material attributes for modelling concrete, along with supplementary concrete material properties, for replicating actual concrete behaviour (Manual 2014).

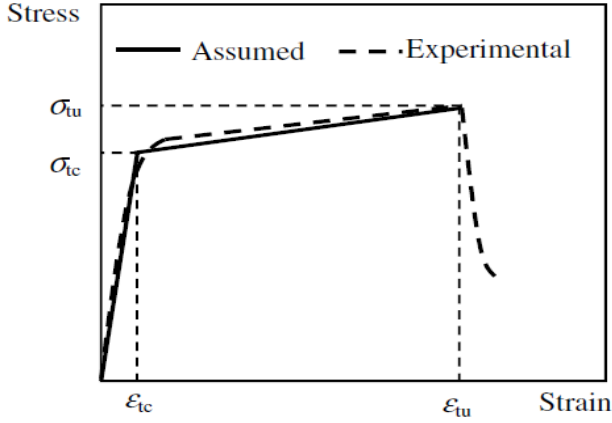
The state of cracked surface is indicated through the shear transfer coefficient  $\beta_s$ , whose value ranges from 0.0 to 1.0, where 0.0 symbolizes a smooth crack while 1.0 represents a coarse crack (Kwan *et al.* 1999, Terec *et al.* 2010). In this study, the value of shear transfer coefficient of an open crack,  $\beta_i$  is 0.2 (Damian *et al.* 2001) while the value of shear transfer coefficient of a closed crack,  $\beta_c$  is 0.8 (Raongjant and Jing 2008). For ECC beams,  $\beta_i=0.05$  and  $\beta_c=0.45$ , were adopted (Wolanski 2004).

The equation  $E_c = 4700\sqrt{f'_c}$ , can be used to calculate the modulus of elasticity of the MSC while the tensile strength can be computed from the equation  $f_r = 0.62\sqrt{f'_c}$ . The Poisson's ratio gave the value of 0.2. Furthermore, the following equations for the multi-linear isotropic stress-strain curve were used to obtain the compressive uniaxial stress-strain values for the MSC model (Damian *et al.* 2001, Raongjant and Jing 2008)

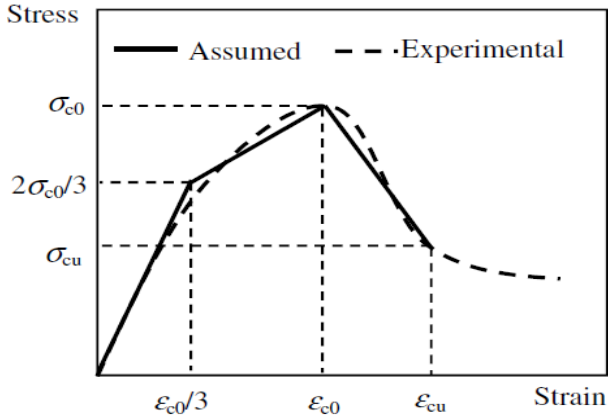
$$E_c = f_{el} / \varepsilon_{el}, \quad \varepsilon_o = \frac{2f'_c}{E_c} \quad \text{and} \quad f = \frac{E_c \varepsilon}{1 + (\varepsilon / \varepsilon_o)^2} \quad (1)$$

Where  $f_{el}$  is the stress at the elastic strain ( $\varepsilon_{el}$ ) in the elastic range ( $f_{el} = 0.30f'_c$ ),  $\varepsilon_o$  is the strain at the ultimate compressive strength,  $\sqrt{f'_c}$  is the compressive strength of the concrete from tests on cylinders and  $f$  is the stress at any strain  $\varepsilon$ .

For ECC, typical stress-strain curves obtained from uniaxial tension and compression tests are shown as dotted lines in Fig. 1 (Kanda *et al.* 2000, Leung and Cao 2010, Zhou *et al.* 2014, Nematollahi *et al.* 2015). To simplify theoretical modeling, the following assumptions which derived by Yuan *et al.* (Yuan *et al.* 2013) were used in this study. These assumptions provide simple analytic formulas for the stress-strain relation of pseudo-strain hardening cementitious composite. The assumption of this approach is



(a) Under uniaxial tension



(b) under uniaxial compression

Fig. 1 Stress-strain relationship of ECC

that fibers are uniformly distributed in the matrix and the fiber reinforced concrete beams is thus modeled as a homogeneous material. It assumes that the main two failure mechanisms are tensile cracking and compressive crushing of the concrete and it allows the definition of strain hardening in compression. The influence of the slag amount, aggregate content, and maximum aggregate size have been considered through the tensile and compressive stresses used in the following assumptions.

The following equations were used to obtain the tensile stress-strain relationship of ECC (Yuan *et al.* 2013)

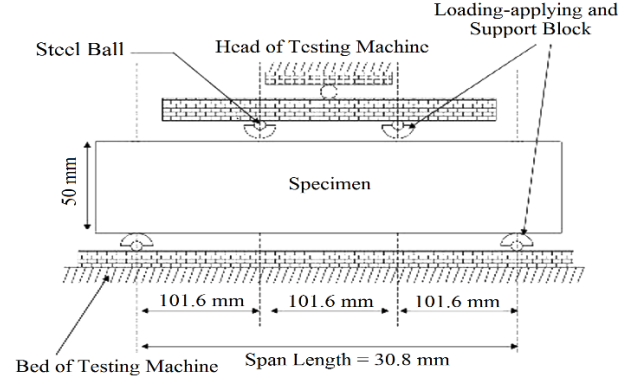
$$\sigma_t = \frac{\sigma_{tc}}{\varepsilon_{tc}} \varepsilon \quad 0 \leq \varepsilon < \varepsilon_{tc} \quad (2)$$

$$\sigma_t = \sigma_{tc} + (\sigma_{tu} - \sigma_{tc}) \left( \frac{\varepsilon - \varepsilon_{tc}}{\varepsilon_{tu} - \varepsilon_{tc}} \right) \quad \varepsilon_{tc} \leq \varepsilon < \varepsilon_{tu} \quad (3)$$

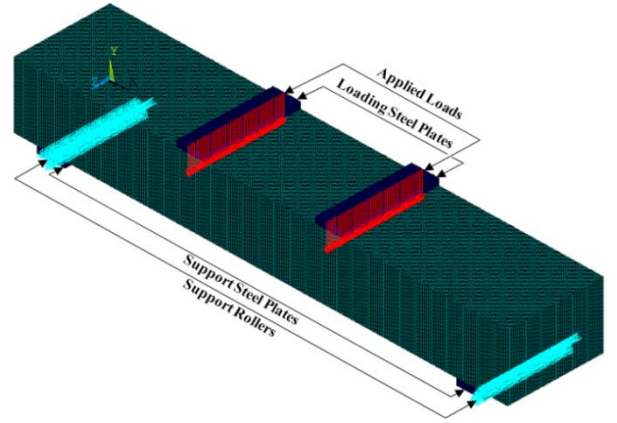
Where  $\sigma_{tc}$  represents the first cracking strength in tension,  $\varepsilon_{tc}$  represents the strain at first cracking,  $\sigma_{tu}$  represents the ultimate tensile strength,  $\varepsilon_{tu}$  represents the tensile strain at  $\sigma_{tu}$ .

The compressive stress-strain relationship of ECC can be expressed as (Yuan *et al.* 2013)

$$\sigma_c = 2 \frac{\sigma_{c0}}{\varepsilon_{c0}} \varepsilon \quad 0 \leq \varepsilon < \frac{1}{3} \varepsilon_{c0} \quad (4)$$



(a) Four-point bending test



(b) Three-dimensional model

Fig. 2 Experimental and numerical specimens

$$\sigma_c = \frac{2}{3} \sigma_{c0} + \frac{\sigma_{c0}}{2\varepsilon_{c0}} \left( \varepsilon - \frac{\varepsilon_{c0}}{3} \right) \quad \frac{1}{3} \varepsilon_{c0} \leq \varepsilon < \varepsilon_{c0} \quad (5)$$

$$\sigma_c = \sigma_{c0} + (\sigma_{cu} - \sigma_{c0}) \left( \frac{\varepsilon - \varepsilon_{c0}}{\varepsilon_{cu} - \varepsilon_{c0}} \right) \quad \varepsilon_{c0} \leq \varepsilon < \varepsilon_{cu} \quad (6)$$

Where  $\sigma_{c0}$  represents the compressive strength,  $\varepsilon_{c0}$  represents the strain at peak stress,  $\sigma_{cu}$  represents the ultimate compressive stress (in the postpeak branch),  $\varepsilon_{cu}$  represents the ultimate compressive strain.

In this study,  $\sigma_{cu}=0.5\sigma_{c0}$  and  $\varepsilon_{cu}=0.5\varepsilon_{c0}$  were adopted. The maximum size of the concrete elements was taken as  $1 \times 1 \times 1$  mm.

Solid 185 element (Manual 2014) were used to model the loading and support plates. The solid element has eight nodes with three degrees of freedom at each node, translations in the nodal  $x$ ,  $y$ , and  $z$  directions. The steel plates incorporated into the finite element models were assumed to be linearly elastic materials with an elastic modulus of 200 GPa and a poisson's ratio of 0.3.

## 2.2 Structural models

In order to study the flexural behaviour of ECC beams, six ECC beams with dimensions of  $(360 \times 75 \times 50)$  mm, have been modelled and compared with MSC beam model, as shown in Fig. 2. The beams were designed to be simply supported over a clear span of 304 mm and subjected to

Table 1 ECC mixture proportions containing slag by weight

Specimen ID.	Cement	$w/b$	Aggregate/Binder		S/C	HRWR ( $\text{kg}/\text{m}^3$ )
			0-400	0-1000		
			$\mu\text{m}$	$\mu\text{m}$		
S-1.2-0.36-400	1	0.27	0.36	-	1.2	5.8
S-1.2-0.45-400	1	0.27	0.45	-	1.2	5.9
S-1.2-0.55-400	1	0.27	0.55	-	1.2	6.0
S-1.2-0.36-1000	1	0.27	-	0.36	1.2	4.9
S-1.2-0.45-1000	1	0.27	-	0.45	1.2	5.0
S-1.2-0.55-1000	1	0.27	-	0.55	1.2	5.0
S-2.2-0.36-400	1	0.27	0.36	-	2.2	4.7
S-2.2-0.45-400	1	0.27	0.45	-	2.2	4.1
S-2.2-0.55-400	1	0.27	0.55	-	2.2	4.3
S-2.2-0.36-1000	1	0.27	-	0.36	2.2	3.5
S-2.2-0.45-1000	1	0.27	-	0.45	2.2	3.6
S-2.2-0.55-1000	1	0.27	-	0.55	2.2	4.0

Table 2 Mechanical and geometric properties of PVA fibers

Fiber Type	Nominal Strength (MPa)	Apparent Strength (MPa)	Diameter ( $\mu\text{m}$ )	Length (mm)	Young Modulus (GPa)	Strain (%)	Specific Weight ( $\text{kg}/\text{m}^3$ )
PVA	1620	1092	39	8	42.8	6.0	1300

four-point loading. The basic mixture ingredients in ECC were: two different fine aggregate sizes (400 and 1000)  $\mu\text{m}$ , three aggregate contents (0.36, 0.45, and 0.55 A/B), Slag (S) mineral admixture type, (1.2 & 2.2 S/C ratio) mineral admixture replacement rate and a constant water-binder ratio ( $w/b$ ) of 0.27 are considered. Details of this factorial design and designation of mixtures are presented in Table 1. PVA fiber 8 mm in length and 39 $\mu\text{m}$  in diameter extensively used in this study. To account for material inhomogeneity, a PVA fiber content of 2% by volume has been typically used in the mixture design. Table 2 illustrates the mechanic and geometric properties of PVA fibers. All the used data in this study based on confirmed experimental results, which have been achieved by (Sahmaran, Yucel *et al.* 2012).

### 3. Verification of numerical modelling with experimental results

#### 3.1 Load-deflection curves

The flexural load-midspan beam deflection curves for all the ECC beams are shown in Fig. 3. In the flexural load-deflection curves, the load at the first drop associated with the first cracking is defined as the first cracking load, the maximum load is defined as the flexural load, and the corresponding deflection is defined as the flexural deflection (midspan beam deflection) capacity. Fig. 3 further shows that while operating under deflecting load, an ECC beam having 1.2 replacement rate of slag bends similar to that of a ductile metal plate due to its property of plastic deformation. In all ECC beams, the flexural cracks prevailing at the tension surface are the first cracks to

appear. Following this, the load increases along with producing multiple cracking, enhancing the inelastic deformation with an increase in stress. Microcracks produced from the first cracking point continued to extend in the midspan of the flexural beam. However, upon reaching the certain limit of fibre strength of the microcracks, bending failure in ECC took place, leading to cause a particular extent of deflection in that part when it reached its limit of flexural strength.

The average first-crack load of ECC beam varies from 1480 to 1630 N in accordance with slag amount. The increase in the S/C ratio from 1.2 to 2.2 reduces the first-crack load by an average of up to 10%. However, aggregate amount have little or no influence on the magnitude of the first-crack load of the ECC beams. Also, the stiffness of the beams does not appear highly sensitive to maximum aggregate size at a given aggregate content. This result is consistent with what is stated in the previous researches (Hind *et al.* 2016a, Aitcin and Mehta 1990, Baalbaki *et al.* 1991, Cetin and Carrasquillo 1998).

#### 3.2 Flexural strength

The numerical flexural strength data for all ECC beams have been studied and compared with MSC beam as shown in Fig. 4. The predicted stress values firstly increase linearly with corresponding deflection before first cracking stress of 9.3 MPa for 400  $\mu\text{m}$  maximum aggregate size beams and 8.1 MPa for 1000  $\mu\text{m}$  maximum aggregate size beams. After that, the curve suddenly changed and keeps almost horizontal until ultimate moment capacity is reached.

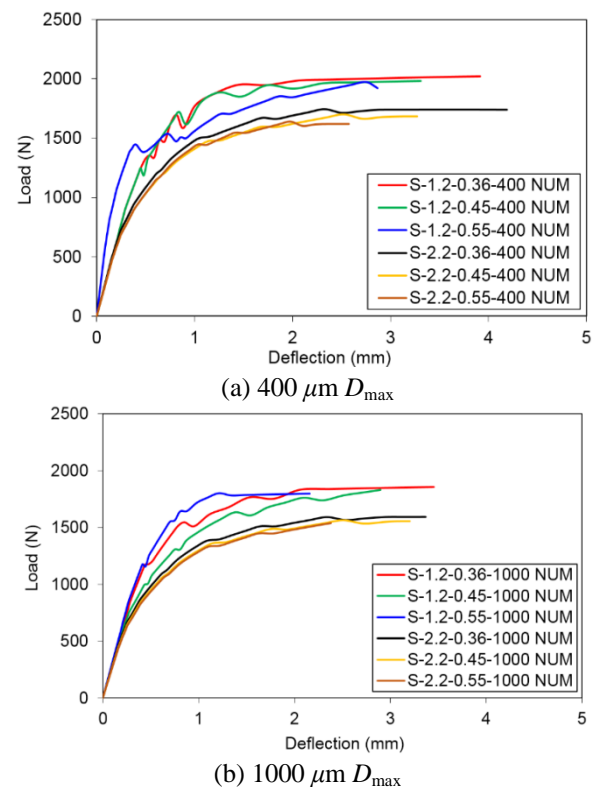


Fig. 3 Numerical flexural load-deflection curves of ECC beams

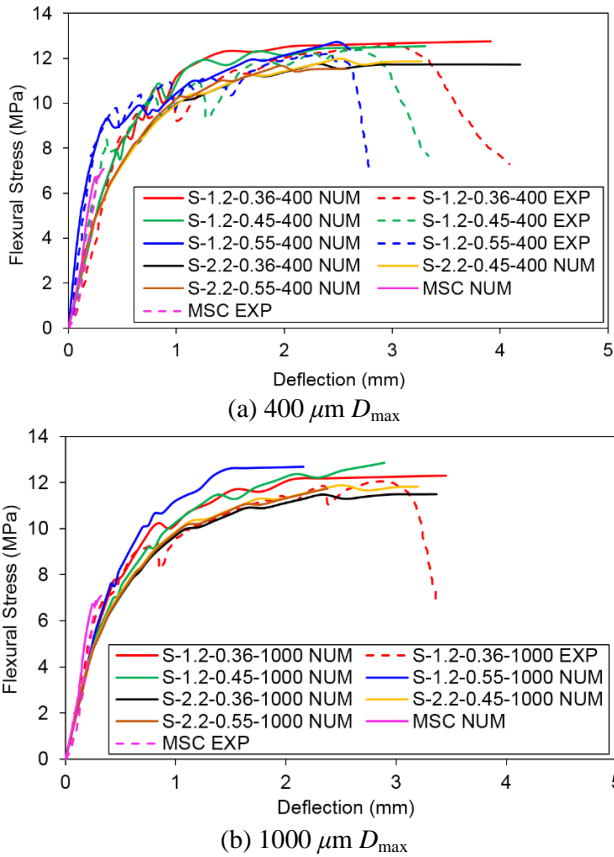


Fig. 4 Comparison between numerical and experimental flexural stress-deflection curves of ECC and MSC beams

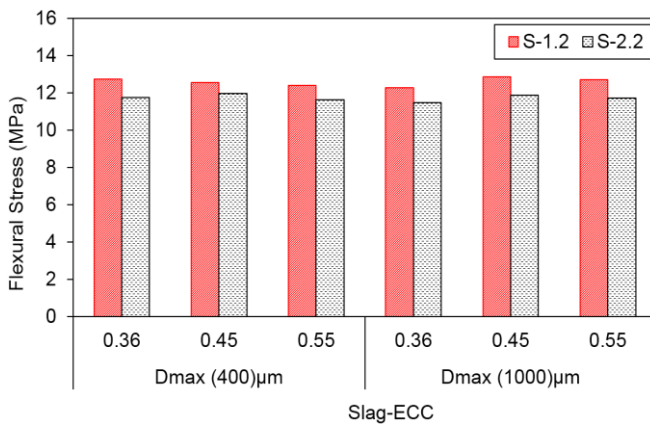


Fig. 5 Influence of slag amount and aggregate size and amount on flexural stress

Fig. 5 shows that the averaged ultimate flexural strengths vary from 11.48 to 12.85 MPa for numerical results. As in the case of compressive strength results, the aggregate content and maximum aggregate size also appear to have a negligible effect on the flexural strength, at least within the parametric range investigated in experimental and numerical studies. Also, the results showed that the increase in the slag amount reduces the ultimate flexural stress in accordance with the maximum aggregate size which match the experimental results.

It is evident that the stresses of beam are decreased by the increase in slag amount and aggregate content and size

as per the contour plots of the simulation results of flexural stress shown in Fig. 6. The cracks continued to spread over the top layer of the beam after cracking, without noticeable crack width. The constant moment region was also surrounded by various minute cracks with parallel to the

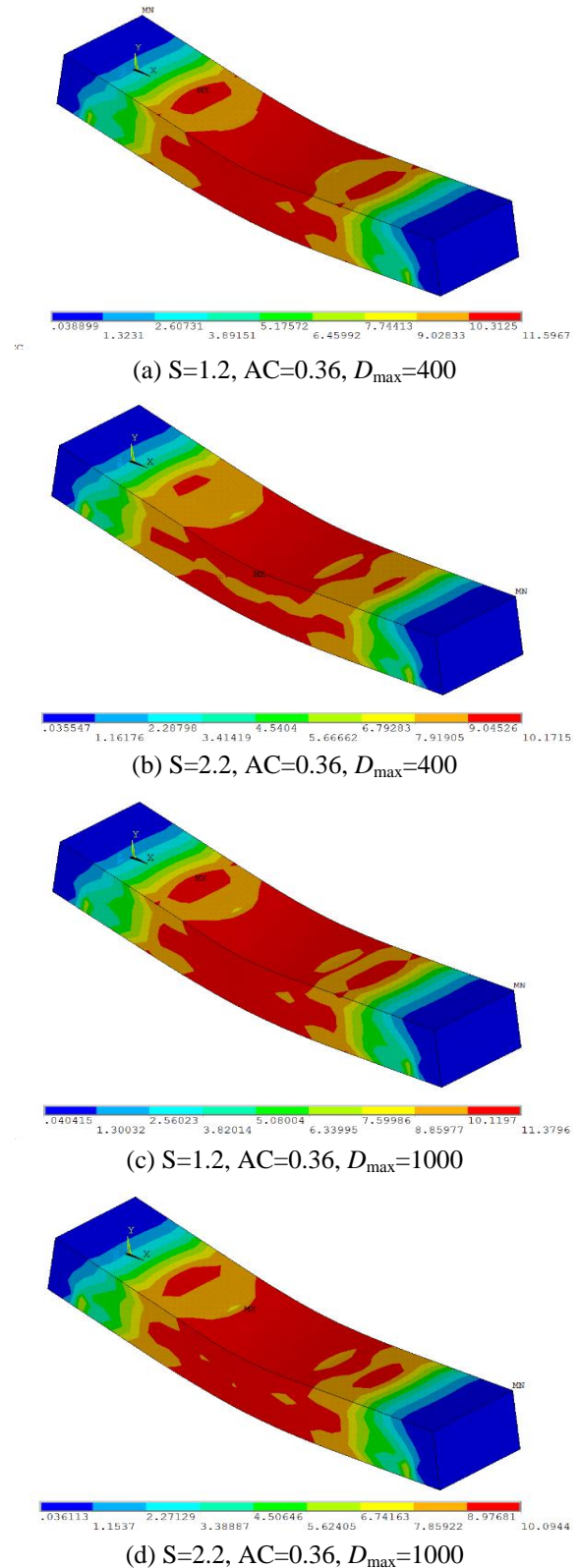


Fig. 6 Contour plots of flexural stress for ECC beams

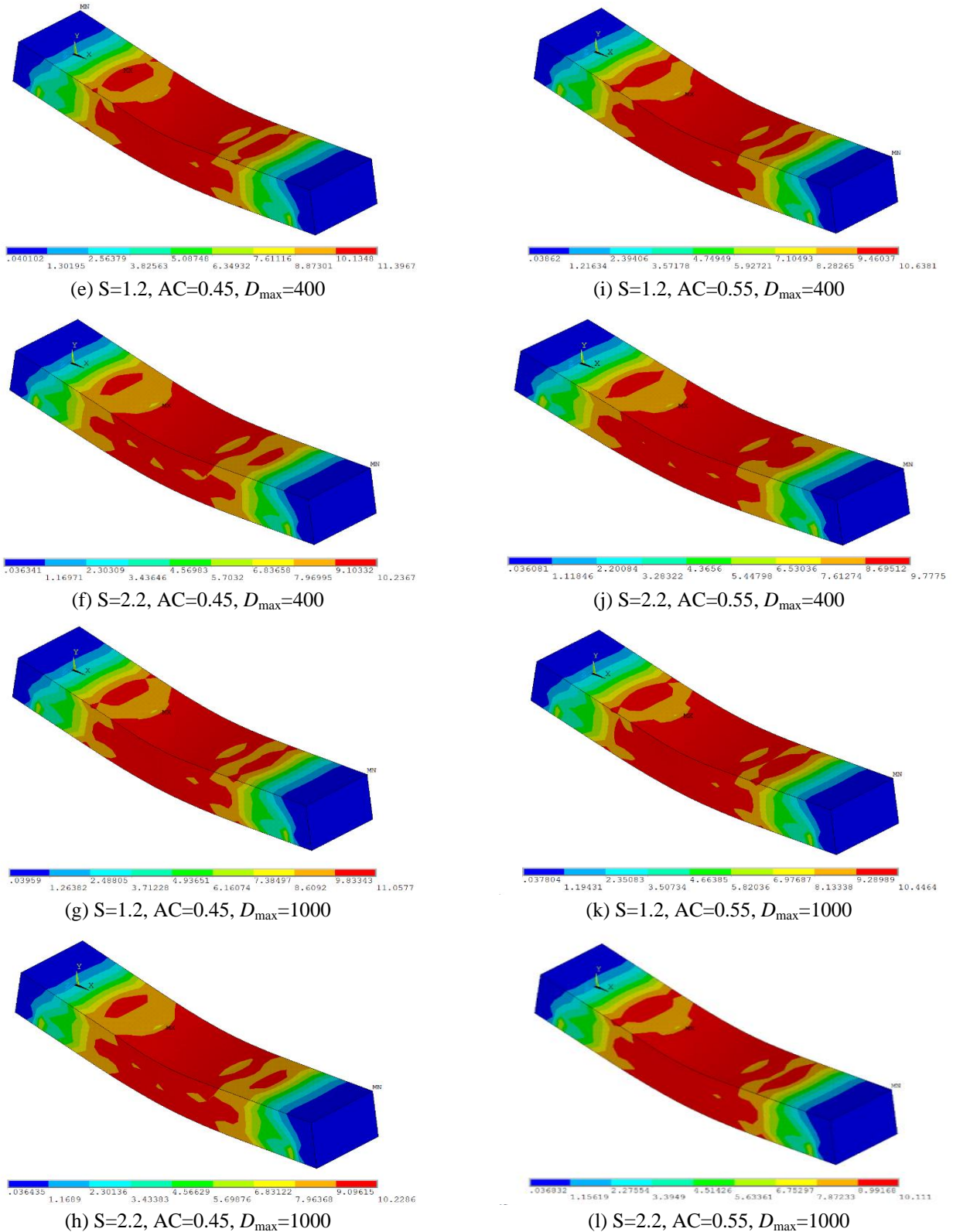


Fig. 6 Continued

major one. At the same time, amid the loading process the division of various minute cracks is also starting from the centre to both supports of the beams. After initial cracking, several cracking along the specimens and minor strain hardening behaviour is quite evident. Following that, the

external moment causes to distort the adhering of fibres and cementitious matrix reducing their ability to withstand the tensile stresses. In this stage the load was continues to decrease gradually once the maximum load is applied. In the end, the ECC beams failed to sustain the stress, leading

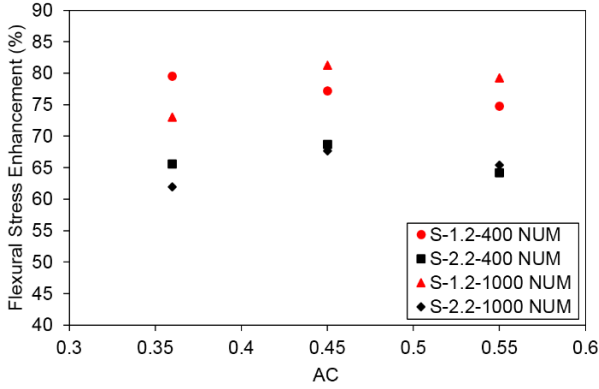


Fig. 7 Flexural stress enhancement versus aggregate content of ECC beams

to cause multiple fibre fracture, giving rise to major cracks in the midspan (Hind *et al.* 2016a, Pan *et al.* 2015).

It appears from Fig. 7 that the ECC beams show enhancement in terms of flexural stress when compared with MSC beam. The average percentage strength improvement of S/C ratio of 1.2 ECC beams as compared to that of MSC beam was 71.51%. While for S/C ratio of 2.2 ECC beams, the average enhancement percentage in flexural stress was 65.59%.

### 3.3 Flexural strain

A numerical flexural stress- strain curve is shown in Fig. 8, which can be parted into two sections:

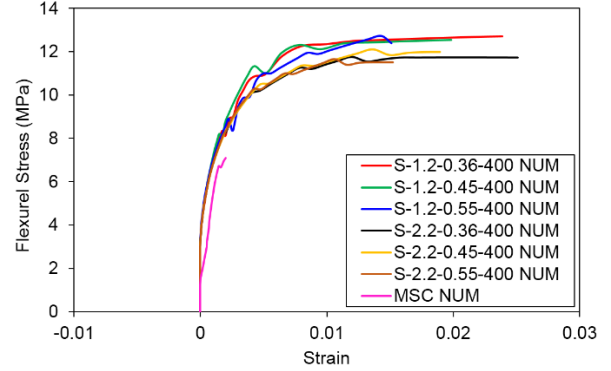
1. Elastic stage: This occurs along the first cracking process. The point of first cracking is analogous to the end of the initial linear section of the stress-strain curve. The strain at this stage is called first cracking strain.
2. Strain hardening stage: In this stage the flexural load-carrying ability increases to cause a consequent increase in strain which is accompanied by multiple cracking. The strain at this stage is called flexural strain.

The average ultimate strain for slag replacement ratio of 1.2 & 2.2 ECC beams are 800% and 650% higher than that from MSC beam, respectively.

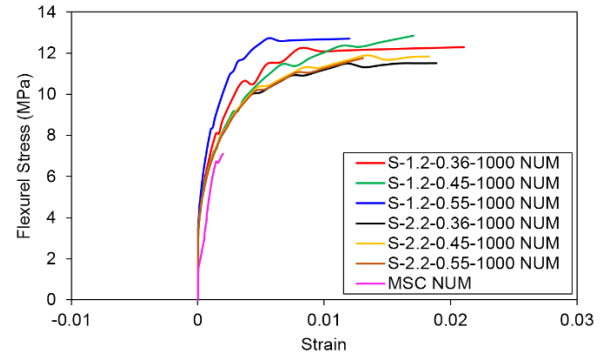
As seen from Fig. 9, the maximum strain and deflection decrease with an increase in slag amount and aggregate content of ECC beams by percentage of 20% and 10%, respectively. Specifically, high aggregate content and the presence of coarse aggregates in a paste tend to increase the matrix (ECC without fiber) toughness, which delays crack initiation and prevents steady-state flat-crack propagation, resulting in a loss of tensile ductility of ECC (Nallathambi *et al.* 1984, Li *et al.* 1995, Perdikaris and Romeo 1995). Furthermore, employing aggregates having a particle size larger than the average fibre spacing may cause balling of fibres, leading to provide inadequate fibre dispersion uniformity (Nagi and Hsu 1992, De Koker and Van Zijl 2004).

### 3.4 Mid-span beam deflection

The flexural deflection capacity of ECC beams, which reflects the material ductility, is summarized in Fig. 10. As



(a) 400  $\mu\text{m}$   $D_{\text{max}}$



(b) 1000  $\mu\text{m}$   $D_{\text{max}}$

Fig. 8 Numerical flexural stress-strain curves of ECC and MSC beams

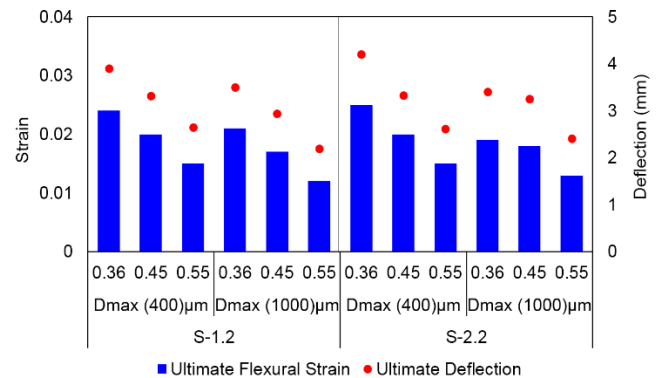


Fig. 9 Influence of slag amount and aggregate size and content on the flexural strain and deflection of ECC beams

shown in this figure, the total deflection of the ECC beam strongly depends on the type and amount of mineral admixture. Beams of S-ECC showed significantly good deflection capacity when compared to the MSC beam. The improvement in the deflection capacity with the use of S can be attributed to the fact that the addition of S has a tendency to reduce PVA fiber/matrix interface chemical bond and matrix (ECC without fiber) toughness while increasing the interface frictional bond (Li 1993).

The adverse effects of increased size of aggregates on ductility performances of ECC are shown in Fig. 10. This figure indicates that the increase in aggregate size and amount result in a decrease in the ECC ductility. The negative effects of increasing aggregate size at large aggregate content on ductility may be attributed to the

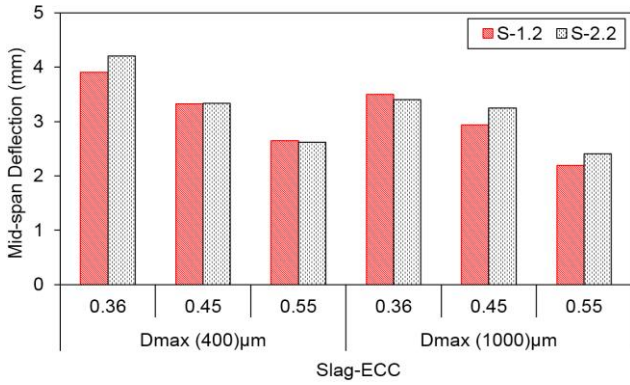


Fig. 10 Influence of slag amount and aggregate size and amount on deformability of ECC beams in flexure

corresponding poor dispersion of fibers. Required coating of fibres by the matrix is avoided by the balling of fibres supported by coarser aggregates at continuous aggregate content. Therefore, this affects a significant component that affects ductility i.e., effective fibre content (Nagi and Hsu 1992). In addition, a greater extent of aggregate interconnection is anticipated for ECCs with larger aggregate size and volume, giving out a greater matrix toughness, which results in the decrease in the margin to develop multiple cracking (Li *et al.* 1995, Li 1998).

It appears from Fig. 11 that the ECC beams show enhancement in terms of deflection when compared with MSC beam. The average percentage deflection enhancement of S/C ratio of 1.2 ECC beams whereas that of MSC beams was 894.79%, while for S/C ratio of 2.2 ECC beams the average percentage deflection enhancement was 863.5%.

Other than ECC properties, characteristics and kinds of mineral admixture plus amount of the PVA fibres also determine the flexural behaviour of the beam specimens. Nonetheless, appropriate and suitable estimates of experimental outcomes can be provided by the simulation outcomes. It is to be noted that the techniques that are used to examine the flexural behaviour of the ECC are tested before they are implemented. The suggested numerical mechanism will be employed to evaluate the impacts of various parameters on the mechanical behaviour of the ECC beams.

#### 4. Nonlinear parametric study

A nonlinear parametric study is carried out to evaluate the influence of parameters on the prediction of the flexural stress, deflection, load and strain of ECC beams in a 3D FE simulation, which comprises aggregate content (AC), ECC compressive strength ( $f_{ECC}$ ), maximum aggregate size ( $D_{max}$ ) and slag amount ( $\phi$ ). These parameters have been obtained using an exponential regression line. The exponential regression analysis resulted in higher  $R^2$  values (0.98) than other types of regression. This type of regression was used because it yielded a more realistic prediction of the flexural behavior of ECC beams (Hind *et al.* 2016e).

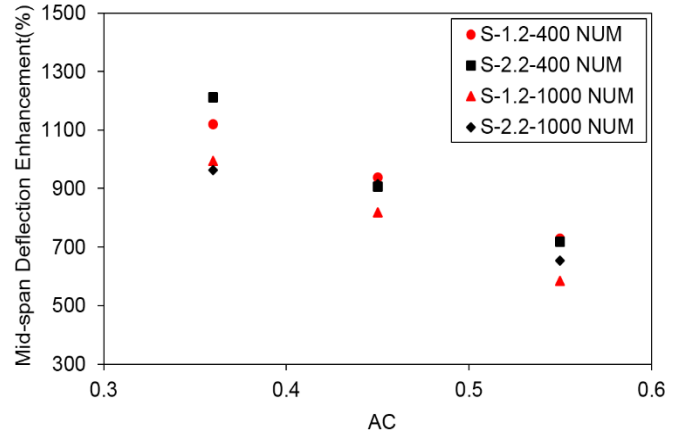


Fig. 11 Deflection enhancement versus aggregate content of ECC beams

#### 4.1 Influence of ECC compressive strength

The compressive strength is an important factor in the stiffness of the ECC beams. Figs. 12 and 13 clarify the influence of the compressive strength on the likelihood of flexural stress and load, where, an increase in the compressive strength increases the flexural stress and load of ECC beams by  $7.13e^{0.006f_{ECC}}$  and  $5.7 \times 10^{-2} e^{0.013f_{ECC}}$ , respectively. Furthermore, the flexural deflection for ECC beams decrease with an increase in compressive strength by  $4.692e^{-0.005f_{ECC}}$ , while the flexural strain increase with an increase in compressive strength by  $0.02e^{-0.001f_{ECC}}$  as shown in Figs. 14 and 15.

#### 4.2 Prediction of new models

It is a well agreed notion that an ideal design of the ECC mixture having its factors in accordance with the micromechanical design theory necessarily requires to be an effective tool able to enhance the mechanical characteristics of hardened mixtures. However, there still exists the need to obtain comprehensive and precise information explaining the mechanical nature of ECC beams as per the provided conditions. Hence, to analyse the ultimate flexural stress ( $FS$ ), deflection ( $Def$ ), load ( $L$ ) and strain ( $ST$ ) statistically, new models of correspondence have been designed on the basis of four major factors of ECC i.e., aggregate content (AC), ECC compressive strength ( $f_{ECC}$ ), maximum aggregate size ( $D_{max}$ ) and slag amount ( $\phi$ ). Eqs. (7)- (10) illustrate these relations

$$FS = \frac{6.532 AC^{-0.012} D_{max}^{0.001}}{f_{ECC}^{-0.152} \phi^{0.089}} \quad (7)$$

$$Def = \frac{7.134 AC^{-0.937} D_{max}^{-0.139}}{f_{ECC}^{0.16} \phi^{-0.032}} \quad (8)$$

$$L = \frac{2.9 AC^{-0.106} D_{max}^{-0.086}}{f_{ECC}^{-0.016} \phi^{0.252}} \times 10^3 \quad (9)$$

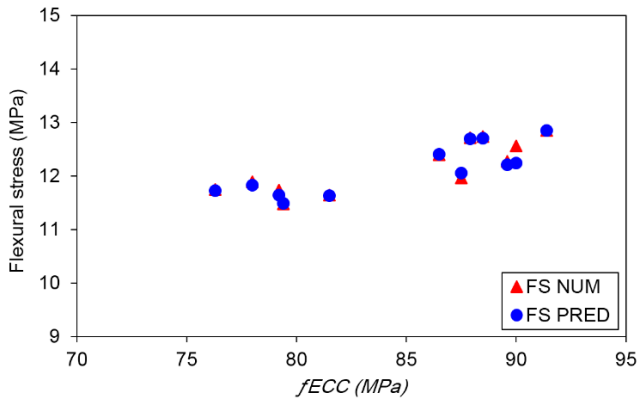


Fig. 12 Influence of ECC compressive strength on the flexural stress by comparing numerical, and predicted results of ECC beams

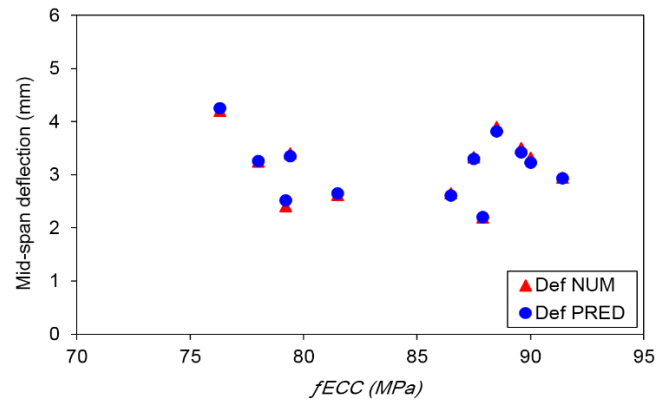


Fig. 14 Influence of ECC compressive strength on the deformability in flexure by comparing numerical, and predicted results of ECC beams

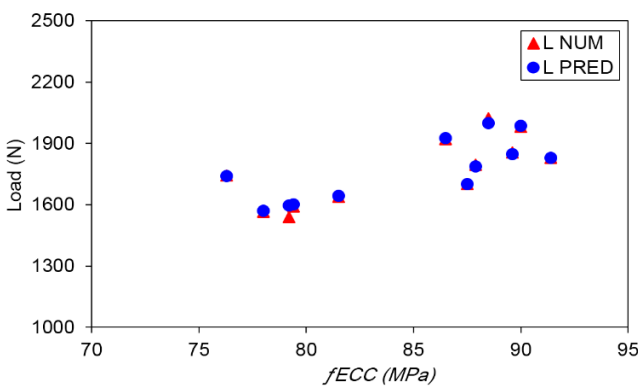


Fig. 13 Influence of ECC compressive strength on the flexural load by comparing numerical, and predicted results of ECC beams

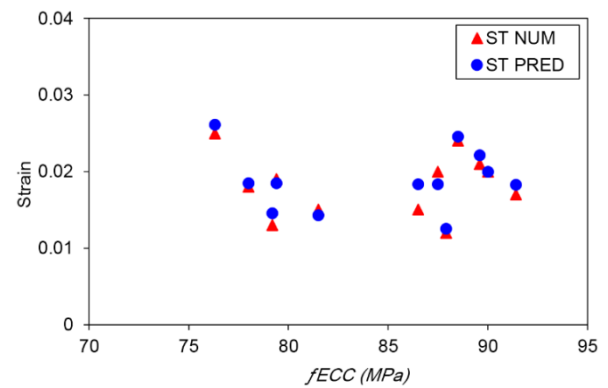


Fig. 15 Influence of ECC compressive strength on the flexural strain by comparing numerical, and predicted results of ECC beams

$$ST = \frac{0.009 AC^{-1.084} D_{\max}^{-0.192}}{f_{ECC}^{-0.221} \phi^{-0.049}} \quad (10)$$

Other than ECC properties, characteristics and types of mineral admixture plus amount of the PVA fibres also determine the flexural behaviour of the beam specimens. Nonetheless, appropriate and suitable estimates of experimental results can be provided by the parametric study results. The provided models may also be employed to obtain a precise estimate of the flexural behaviour of ECC beams.

## 5. Conclusions

This research aims to analyse the potential effect of aggregate size and amount upon the mechanical performances of ECC beams by means of employing nonlinear finite element model. To test the validity of models of the ECC beams operating under monotonic loading, experimental results were obtained. Based on the numerical analysis method, nonlinear parametric study was then conducted to evaluate the influence of the aggregate content ( $AC$ ), ECC compressive strength ( $f_{ECC}$ ), maximum aggregate size ( $D_{\max}$ ) and slag amount ( $\phi$ ) on the flexural

stress, deflection, load and strain of ECC beams. From the results obtained, the following conclusions can be drawn:

- The simulation results indicate that when increase the aggregate size and content no definite trend in flexural strength is observed, at least for the limited aggregate size range studied. The ductility of ECC is negatively influenced by the increase of slag and aggregate size and content.
- The ECC beams showed enhancement in terms of flexural stress, strain, and midspan deflection when compared with MSC beam, where, the average improvement percentage of the specimens were 61.55%, 725%, and 879%, respectively.
- As per the finite element analysis, the flexural stress-deflection property of the beams was in agreement with the results obtained from experiments. Nonetheless, the numerical values for average ultimate strength and deflection obtained for the beams are 1.6% larger than those obtained from the experimental results. In addition to the ECC properties, the flexural behaviour of the beam can also be identified through properties and nature of mineral admixture, and quantity of the PVA fibres. The accuracy of experimental results can only be obtained through replication of results. Furthermore, the numerical method to identify the flexural behaviour of the ECC beams is validated through these results.

- The nonlinear parametric study demonstrated that the mid-span beam deflection properties, through which material ductility, flexural stress, load and strain of ECC beams are subjected to considerable variations with respect to changes in  $AC$ ,  $D_{max}$ ,  $f_{ECC}$  and  $\phi$  parameters. The deflection ability and flexural stress of the beams are in a negative relation with these factors.

## Acknowledgments

The researchers gratefully acknowledge the technical support provided by Faculty of Civil Engineering at University of Gaziantep.

## References

- Aitcin, P.C. and Mehta, P.K. (1990), "Effect of coarse aggregate characteristics on mechanical properties of high-strength concrete", *ACI Mater. J.*, **87**(2), 103-107.
- Baalbaki, W., Benmokrane, B., Chaallal, O. and Aitcin, P.C. (1991), "Influence of coarse aggregate on elastic properties of high-performance concrete", *ACI Mater. J.*, **88**(5), 499-503.
- Balaguru, P.N. and Shah, S.P. (1992), *Fiber-reinforced Cement Composites*.
- Cetin, A. and Carrasquillo, R.L. (1998), "High-performance concrete: influence of coarse aggregates on mechanical properties", *ACI Mater. J.*, **95**(3), 252-261.
- Cho, C.G., Kim, Y.Y., Feo, L. and Hui, D.V. (2012), "Cyclic responses of reinforced concrete composite columns strengthened in the plastic hinge region by HPFRCC mortar", *Compos. Struct.*, **94**(7), 2246-2253.
- D'Ambrisi, A., Feo, L. and Focacci, F. (2012), "Bond-slip relations for PBO-FRCM materials externally bonded to concrete", *Compos. Part B-Eng.*, **43**(8), 2938-2949.
- D'Ambrisi, A., Feo, L. and Focacci, F. (2013), "Experimental analysis on bond between PBO-FRCM strengthening materials and concrete", *Compos. Part B-Eng.*, **44**(1), 524-532.
- Damian, K., Thomas, M., Solomon, Y., Kasidit, C. and Tanarat, P. (2001), "Finite element modeling of reinforced concrete structures strengthened with FRP laminates", Report for Oregon Department Of Transportation, Salem.
- De Koker, D. and Van Zijl, G. (2004), "Extrusion of engineered cement-based composite material", *Proceedings of the 6th RILEM Symposium on Fiber-Reinforced Concretes (FRC)*.
- Dhawale, A. and Joshi, V. (2013), "Engineered cementitious composites for structural applications", *Int. J. Appl. Innov. Eng. Manage.*, **2**, 198-205.
- Fischer, G. and Li, V.C. (2003), "Deformation behavior of fiber-reinforced polymer reinforced engineered cementitious composite (ECC) flexural members under reversed cyclic loading conditions", *ACI Mater. J.*, **100**(1), 25-35.
- Fraternali, F., Ciancia, V., Chechile, R., Rizzano, G., Feo, L. and Incarnato, L. (2011), "Experimental study of the thermo-mechanical properties of recycled PET fiber-reinforced concrete", *Composite Structures*, **93**(9), 2368-2374.
- Hawileh, R.A. (2015), "Finite element modeling of reinforced concrete beams with a hybrid combination of steel and aramid reinforcement", *Mater. Des.*, **65**, 831-839.
- Hind, M.K., Özakça, M. and Ekmekyapar, T. (2016b), "Numerical and parametric studies on flexural behavior of ECC beams by considering the effect of slag and micro-PVA fiber", *J. Adv. Res. Appl. Mech.*, **1**(21), 1-21.
- Hind, M.K., Özakça, M. and Ekmekyapar, T. (2016c), "A review on nonlinear finite element analysis of reinforced concrete beams retrofitted with fiber reinforced polymers", *J. Adv. Res. Appl. Mech.*, **1**(22), 13-48.
- Hind, M.K., Özakça, M. and Ekmekyapar, T. (2016d), "Numerical and parametric studies on flexural behavior of ECC beams by considering the effect of fly-ash and micro-PVA fiber", *J. Adv. Res. Appl. Sci. Eng. Tech.*, **1**(3), 48-66.
- Hind, M.K., Özakça, M., Abdolbaqi, M.K. and Ekmekyapar, T. (2016e), "Flexural performance of PVA reinforced ECC beams: numerical and parametric studies", *The Third National Conference for Postgraduate Research (NCON-PGR2016)*, Pahang, Malaysia, September.
- Hind, M.K., Ozakca, M., Ekmekyapar, T. and Abdolbaqi, M.K. (2016a), "Flexural behavior of concrete beams reinforced with different types of fibers", *Comput. Concrete*, **18**(5), 999-1018.
- Kanda, T., Lin, Z. and Li, V.C. (2000), "Tensile stress-strain modeling of pseudostrain hardening cementitious composites", *J. Mater. Civil Eng.*, **12**(2), 147-156.
- Kim, J.K., Kim, J.S., Ha, G.J. and Kim, Y.Y. (2007), "Tensile and fiber dispersion performance of ECC (engineered cementitious composites) produced with ground granulated blast furnace slag", *Cement Concrete Res.*, **37**(7), 1096-1105.
- Kunieda, M. and Rokugo, K. (2006), "Recent progress on HPFRCC in Japan required performance and applications", *J. Adv. Concrete Technol.*, **4**(1), 19-33.
- Kwan, A., Dai, H. and Cheung, Y. (1999), "Non-linear seismic response of reinforced concrete slit shear walls", *J. Sound Vib.*, **226**(4), 701-718.
- Lepech, M.D. and Li, V.C. (2008), "Large-scale processing of engineered cementitious composites", *ACI Mater. J.*, **105**(4), 358-366.
- Leung, C.K.Y. and Cao, Q.A. (2010), "Development of pseudo-ductile permanent formwork for durable concrete structures", *Mater. Struct.*, **43**(7), 993-1007.
- Li, V. (1993), "From micromechanics to structural engineering-the design of cementitious composites for civil engineering applications", *Struct. Eng. Earthq. Eng. JPN Soc Civil Eng.*, **10**(2), 37-48.
- Li, V. (2002), "Advances in ECC research. Material science to application-a tribute to Surendra P. Shah", *ACI Bookstore*, 73-400.
- Li, V.C. (1993), "From micromechanics to structural engineering-the design of cementitious composites for civil engineering applications", *JSCCE J. Struct. Mech. Earthq. Eng.*, **10**(2), 37-48.
- Li, V.C. (1998), "Engineered cementitious composites-tailored composites through micromechanical modeling", *Fiber Reinforced Concrete: Present and the Future*, Ed. N. Banthia, in *Fiber Reinforced Concrete: Present and the Future*, Eds. N. Banthia, A. Bentur, A. and A. Mufti, Canadian Society for Civil Engineering, Montreal.
- Li, V.C. (1998), "Engineered cementitious composites (ECC)-tailored composites through micromechanical modeling", *Micromechanical, T.C.T.*
- Li, V.C. (2008), "Engineered Cementitious Composites (ECC) material, structural, and durability performance".
- Li, V.C., Mishra, D.K. and Wu, H.-C. (1995), "Matrix design for pseudo-strain-hardening fibre reinforced cementitious composites", *Mater. Struct.*, **28**(10), 586-595.
- Li, V.C., Wang, S. and Wu, C. (2001), "Tensile strain-hardening behavior of polyvinyl alcohol engineered cementitious composite (PVA-ECC)", *ACI Mater. J.*, **98**(6).
- Lim, Y.M. and Li, V.C. (1997), "Durable repair of aged infrastructures using trapping mechanism of engineered cementitious composites", *Cement Concrete Compos.*, **19**(4), 373-385.
- Lin, Z. and Li, V.C. (1997), "Crack bridging in fiber reinforced cementitious composites with slip-hardening interfaces", *J.*

- Mech. Phys. Solid.*, **45**(5), 763-787.
- Lin, Z., Kanda, T. and Li, V.C. (1999), "On interface property characterization and performance of fiber reinforced cementitious composites", *Concrete Sci. Eng.*, **1**(3), 173-184.
- Maalej, M. and Li, V.C. (1995), "Introduction of strain-hardening engineered cementitious composites in design of reinforced concrete flexural members for improved durability", *ACI Struct. J.*, **92**(2).
- Manual, A.U.s. (2014), "Version (15)", Swanson Analysis Systems Inc.
- Maruta, M., Kanda, T., Nagai, S. and Yamamoto, Y. (2005), "New high-rise RC structure using pre-cast ECC coupling beam", *Concrete J.*, **43**(11), 18-26.
- Nagi, M. and Hsu, J.W. (1992), "Optimization of the use of lightweight aggregates in carbon fiber reinforced cement", *ACI Mater. J.*, **89**(3), 267-276.
- Nallathambi, P., Karihaloo, B. and Heaton, B. (1984), "Effect of specimen and crack sizes, water/cement ratio and coarse aggregate texture upon fracture toughness of concrete", *Magf Concrete Res.*, **36**(129), 227-236.
- Nematollahi, B., Sanjayan, J. and Ahmed Shaikh, F.U. (2015), "Tensile strain hardening behavior of PVA fiber-reinforced engineered geopolymer composite", *J. Mater. Civil Eng.*, 04015001.
- Pan, Z.F., Wu, C., Liu, J.Z., Wang, W. and Liu, J.W. (2015), "Study on mechanical properties of cost-effective polyvinyl alcohol engineered cementitious composites (PVA-ECC)", *Constr. Build. Mater.*, **78**, 397-404.
- Perdikaris, P.C. and Romeo, A. (1995), "Size effect on fracture energy of concrete and stability issues in three-point bending fracture toughness testing", *ACI Mater. J.*, **92**(5), 483-496.
- Raongiant, W. and Jing, M. (2008), "Finite element analysis on lightweight reinforced concrete shear walls with different web reinforcement", *The Sixth Prince of Songkla Univ. Engng. Conference*, Hat Yai, Thailand.
- Sahmaran, M. and Li, V.C. (2009), "Influence of microcracking on water absorption and sorptivity of ECC", *Mater. Struct.*, **42**(5), 593-603.
- Şahmaran, M., Bilici, Z., Ozbay, E., Erdem, T.K., Yucel, H.E. and Lachemi, M. (2013), "Improving the workability and rheological properties of engineered cementitious composites using factorial experimental design", *Compos. Part B: Eng.*, **45**(1), 356-368.
- Şahmaran, M., Lachemi, M., Hossain, K.M., Ranade, R. and Li, V.C. (2009), "Influence of aggregate type and size on ductility and mechanical properties of engineered cementitious composites", *ACI Mater. J.*, **106**(3), 308-316.
- Sahmaran, M., Yucel, H.E., Demirhan, S., Ank, M.T. and Li, V.C. (2012), "Combined effect of aggregate and mineral admixtures on tensile ductility of engineered cementitious composites", *ACI Mater. J.*, **109**(6), 627-637.
- Said, S.H. and Razak, H.A. (2015), "The effect of synthetic polyethylene fiber on the strain hardening behavior of engineered cementitious composite (ECC)", *Mater. Des.*, **86**, 447-457.
- Said, S.H., Razak, H.A. and Othman, I. (2015), "Flexural behavior of engineered cementitious composite (ECC) slabs with polyvinyl alcohol fibers", *Construction and Building Materials*, **75**, 176-188.
- Terec, L., Bugnariu, T. and Pastrav, M. (2010), "Non-linear analysis of reinforced concrete frames strengthened with infilled walls", *Rev. Rom. Mater.*, **40**(3), 214-221.
- Wang, S.X. and Li, V.C. (2007), "Engineered cementitious composites with high-volume fly ash", *ACI Mater. J.*, **104**(3), 233-241.
- Wolanski, A.J. (2004), *Flexural Behavior of Reinforced and Prestressed Concrete Beams using Finite Element Analysis*, Citeseer.
- Yang, D.S., Park, S.K. and Neale, K.W. (2009), "Flexural behaviour of reinforced concrete beams strengthened with prestressed carbon composites", *Compos. Struct.*, **88**(4), 497-508.
- Yuan, F., Pan, J. and Leung, C. (2013), "Flexural behaviors of ECC and concrete/ECC composite beams reinforced with basalt fiber-reinforced polymer", *J. Compos. Constr.*, **17**(5), 591-602.
- Zhang, J. and Li, V.C. (2002), "Monotonic and fatigue performance in bending of fiber-reinforced engineered cementitious composite in overlay system", *Cement Concrete Res.*, **32**(3), 415-423.
- Zhang, J., Leung, C.K.Y. and Cheung, Y.N. (2006), "Flexural performance of layered ECC-concrete composite beam", *Compos. Sci. Technol.*, **66**(11-12), 1501-1512.
- Zhou, J., Pan, J. and Leung, C. (2014), "Mechanical behavior of fiber-reinforced engineered cementitious composites in uniaxial compression", *J. Mater. Civil Eng.*, **27**(1), 04014111.
- Zhou, J., Qian, S., Beltran, M.G.S., Ye, G., van Breugel, K. and Li, V.C. (2010), "Development of engineered cementitious composites with limestone powder and blast furnace slag", *Mater. Struct.*, **43**(6), 803-814.

CC